Acta Crystallographica Section D
Biological Crystallography
ISSN 0907-4449

Crystallization of the catalytic subunit of *Saccharomyces cerevisiae* acetohydroxyacid synthase

S. S. Pang, L. W. Guddat and R. G. Duggleby*

Centre for Protein Structure, Function and Engineering, Department of Biochemistry and Molecular Biology, School of Molecular and Microbial Sciences, The University of Queensland, Brisbane, QLD 4072, Australia

Correspondence e-mail: duggleby@biosci.uq.edu.au

Received 27 March 2001
Accepted 10 July 2001

Acetohydroxyacid synthase (AHAS; E.C. 4.1.3.18) is the first enzyme in the biosynthetic pathway of the branched-chain amino acids isoleucine, leucine and valine. It is a thiamin diphosphate-dependent enzyme which catalyses the decarboxylation of pyruvate and its condensation with either 2-ketobutyrate or a second molecule of pyruvate to give 2-aceto-2-hydroxybutyrate or 2-acetolactate, respectively. The enzyme is the target of sulfonylurea and imidazolinone herbicides, which act as potent and specific inhibitors. Here, the crystallization and preliminary X-ray diffraction analysis of the catalytic subunit of *Saccharomyces cerevisiae* AHAS is reported. Data to 2.7 Å resolution have been collected using synchrotron radiation (Advanced Photon Source, Chicago). Crystals have unit-cell parameters $a = 95.8$, $b = 110.0$, $c = 178.9$ Å and belong to the space group $P2_12_12_1$. Preliminary analysis indicates there is one dimer located in each asymmetric unit.

1. Introduction

Acetohydroxyacid synthase (AHAS; E.C. 4.1.3.18; reviewed by Duggleby & Pang, 2000), also known as acetolactate synthase, catalyses the decarboxylation of pyruvate and its condensation with either 2-ketobutyrate or a second molecule of pyruvate to give 2-aceto-2-hydroxybutyrate or 2-acetolactate, respectively (Gollop *et al.*, 1989). The product 2-acetolactate is a precursor molecule used in the biosynthesis of valine and leucine, while 2-aceto-2-hydroxybutyrate is the precursor for isoleucine. AHAS belongs to a homologous family of enzymes that cleave a carbon–carbon bond adjacent to a carbonyl group using thiamin diphosphate (ThDP) as a cofactor. In addition to ThDP, which participates directly in catalysis, AHAS requires two other cofactors: a divalent metal ion that is thought to anchor ThDP to the enzyme and flavin adenine dinucleotide (FAD), the function of which is unknown. Interest in AHAS has been stimulated by the fact that this enzyme is the target for several diverse families of herbicides, including sulfonylureas, imidazolinones, triazolopyrimidines and pyriminidinyl oxybenzoates.

It is generally agreed that the bacterial enzyme functions as a multimeric protein. In *Escherichia coli* and *Salmonella typhimurium*, three isozymes of AHAS have been observed and all are tetramers consisting of two catalytic subunits (~60 kDa) and two regulatory subunits (9–17 kDa). The catalytic subunit alone shows low (Weinstock *et al.*, 1992; Vyazmensky *et al.*, 1996) or no activity (Hill *et al.*, 1997) and is greatly stimulated by reconstitution with the regulatory subunit. Moreover, the reconstituted enzyme acquires sensitivity to feedback inhibition by valine. In contrast, a regulatory subunit has never been observed for the enzyme isolated from eukaryotes, although the existence of such a subunit has been inferred from other evidence (Duggleby, 1997).

In 1999, we showed that the open reading frame *YCL009c* corresponds to the yeast AHAS regulatory subunit and that combining the two purified yeast subunits in concentrated phosphate and neutral pH increased the catalytic activity sevenfold compared with the catalytic subunit alone (Pang & Duggleby, 1999). The stimulated activity is sensitive to valine inhibition and this inhibition is reversed by ATP. Later work elsewhere (Hershey *et al.*, 1999) identified a putative tobacco AHAS regulatory subunit and we have described the *Arabidopsis thaliana* equivalent (Lee & Duggleby, 2001). It now seems likely that such subunits are a common feature of AHAS from all species.

No experimentally determined structure of AHAS from any source has been reported. However, the structures of several ThDP-dependent enzymes are known, including *Lactobacillus plantarum* pyruvate oxidase (POX; Muller & Schulz, 1993), *Pseudomonas putida* benzoylformate decarboxylase (BFD; Hasson *et al.*, 1998), pyruvate decarboxylase from *S. uvarum* (Dyda *et al.*, 1993), *S. cerevisiae*

(Arjunan *et al.*, 1996) and *Zymomonas mobilis* (Dobritzsch *et al.*, 1998), *S. cerevisiae* transketolase (Lindqvist *et al.*, 1992; Nikkola *et al.*, 1994), the E1 component of the branched-chain 2-ketoacid dehydrogenase complex from *P. putida* (Ævarsson *et al.*, 1999) and *Homo sapiens* (Ævarsson *et al.*, 2000) and *Desulfovibrio africanus* pyruvate: ferredoxin oxidoreductase (Chabrière *et al.*, 1999). Several of these enzymes exhibit weak homology (up to ∼30% identity) with the catalytic subunit of AHAS, but none of them contain a homologue of the AHAS regulatory subunit. Two homology models for the catalytic subunit of AHAS, based on POX, have been constructed (Ott *et al.*, 1996; Ibdah *et al.*, 1996) and these models have been useful in predicting specific residues involved in catalysis and herbicide binding. Recently, tentative models of the AHAS regulatory subunit have been described (Mendel *et al.*, 2001; Lee & Duggleby, 2001).

Determination of the structure of AHAS will elucidate the geometrical arrangement of the catalytically important residues in the active site and define the structure of the herbicide inhibitor-binding site. Clues to the catalytic mechanism, the control of substrate specificity, the role of FAD, the mode of action of the regulatory subunit and the mechanism of regulation by valine and ATP and ideas as to how improved AHAS inhibitors could be developed should also emerge once the structure is known. In this study, we have crystallized the catalytic subunit of *S. cerevisiae* AHAS in the presence of the three cofactors, Mg^{2+}, ThDP and FAD.

2. Materials and methods

2.1. Expression, purification and preparation

Construction of the expression vector (pET.YLSU) used in the production of the catalytic subunit of AHAS has been described previously (Pang & Duggleby, 1999). The catalytic subunit of AHAS was expressed in *E. coli* strain BL21 (DE3) cells, which were transformed, induced and harvested as described previously (Pang & Duggleby, 1999). Cell lysis and purification of the expressed 6×His-tagged protein was by immobilized metal affinity chromatography (IMAC) as described previously (Pang & Duggleby, 1999), except that after the elution of the catalytic subunit from the IMAC column sufficient potassium phosphate solution pH 6.0 was added to the active fractions to give a final concentration of 0.2 *M*. The molecular weight of the expressed and purified construct was determined by mass spectrometry to be 73 518 Da. This value corresponds to that expected for the recombinant catalytic subunit of AHAS after removal of the mitochondrial transit peptide, a 5 kDa fusion protein containing the 6×His tag and one water molecule. The first crystallization trials were set up with this material, but yielded only small poorly diffracting crystals. To improve the quality of the crystals, an additional gel-filtration purification step was performed using a Superdex HR10/30 size-exclusion FPLC column. The catalytic subunit of AHAS was eluted in buffer that contained 0.2 *M* potassium phosphate pH 6.0, 1 m*M* DTT and 10 µ*M* FAD. For long-term storage, the catalytic subunit of AHAS was concentrated to 12–20 mg ml^{-1} and transferred to a buffer containing 0.2 *M* potassium phosphate pH 6.0, 10 µ*M* FAD and 1 m*M* DTT before being divided into aliquots of 100 µl and flash-frozen in liquid nitrogen.

2.2. Crystallization and data collection

Crystallization trials were performed using the hanging-drop vapour-diffusion method at 293 K. The search for suitable crystallization conditions was carried out using Hampton Crystal Screens I and II. Crystallization conditions were refined by application of the grid-screen approach (Bergfors, 1999). Before each crystallization experiment, the three cofactors and DTT were added to the freshly thawed enzyme aliquot to give final concentrations of 1 m*M* ThDP, 1 m*M* $MgCl_2$, 1 m*M* FAD and 5 m*M* DTT. Optimal crystal growth was obtained by combining 1 µl of the catalytic subunit of AHAS with 1 µl of reservoir solution. The reservoir solution consisted of 14% PEG 4000, 0.25–0.3 *M* potassium phosphate pH 5.8 and 0.2 *M* ammonium acetate. The crystals that appear within 3–4 d are yellow (owing to the bound FAD cofactor) and prismatic in shape and take 14 d to reach their maximum size.

Preliminary X-ray studies on these crystals at room temperature using a rotating-anode generator showed diffraction to ∼3.2 Å resolution. However, the diffraction intensity of the crystals decreased quickly after the initial exposure to X-rays. To overcome this problem, we developed a cryocooling strategy, which involves transfer of the crystals to reservoir solution that has 15%(*v*/*v*) glycerol added for cryoprotection. Crystals were stable in this solution for at least 0.5 h, showing no signs of cracking or dissolving.

A complete data set for the AHAS catalytic subunit crystals was collected using a wavelength of 1.0 Å on beamline 14C at the Advance Photon Source in the Argonne National Laboratory, Chicago, USA. Data images were recorded on a Q4 CCD detector positioned 225 mm from the crystal. Each oscillation frame was 0.3° in width and was exposed for 20 s. The diffraction data were processed to 2.7 Å resolution using the program *DENZO* (Otwinowski & Minor, 1997) and were scaled with the program *SCALEPACK* (Otwinowski & Minor, 1997). Analysis of the X-ray diffraction pattern and averaging of equivalent intensities allowed characterization of the Laue symmetry.

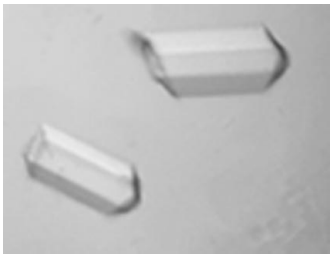

Figure 1
Two crystals of the catalytic subunit of AHAS. The larger one has dimensions of 0.5 × 0.2 × 0.2 mm.

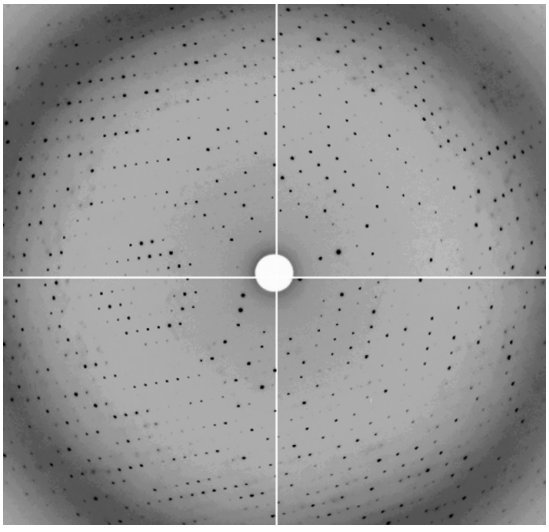

Figure 2
A 0.3° oscillation frame of a cryocooled crystal of the catalytic subunit of AHAS. Diffraction data are observed to 2.7 Å resolution.

Table 1
Data-collection statistics for the catalytic subunit of AHAS.

Values in parentheses are statistics for the 2.81–2.70 Å resolution shell.

Temperature (K)	100
Resolution range (Å)	100.0–2.70
Total No. of observations [$I > 0\sigma(I)$]	188597 (12439)
No. of unique reflections [$I > 0\sigma(I)$]	49759 (4649)
Completeness (%)	95.9 (81.7)
R_{sym}†	0.043 (0.126)
$\langle I\rangle/\langle\sigma(I)\rangle$	22.6 (13.6)

† $R_{sym} = \sum|I - \langle I\rangle|/\sum\langle I\rangle$, where I is the intensity of an individual measurement of each reflection and $\langle I\rangle$ is the mean intensity of that reflection.

3. Results and discussion

The initial series of crystallization trials on the catalytic subunit of AHAS gave drops that contained numerous nucleation sites, resulting in the production of small poorly diffracting crystals. The stored protein is very stable but the IMAC purification procedure would not separate active from inactive AHAS. To solve this problem, an additional gel-filtration step was added to the purification procedure. This had the effect of removing inactive protein from the concentrated solution. Using the standard assay procedure, the specific activity of this highly purified enzyme was 5.0 U mg^{-1} compared with 2.5 U mg^{-1} before gel filtration. Large diffraction-quality crystals of the catalytic subunit of AHAS could now be obtained.

The largest crystals of the catalytic subunit of AHAS have dimensions of 0.5 × 0.2 × 0.2 mm (Fig. 1), diffract to 2.7 Å resolution (Fig. 2), have unit-cell parameters $a = 95.8$, $b = 110.0$, $c = 178.9$ Å and belong to the space group $P2_12_12_1$. The mosaic spread of these crystals at room temperature is 0.23° and increases to 0.35° at 100 K. The volume of the unit cell is 1.885 × 10^6 Å^3. Assuming there is one dimer (∼147 kDa) in the asymmetric unit, the Matthews coefficient (Matthews, 1968) V_M is 3.62 Å^3 Da^{-1}. Based on a value of 0.74 cm^3 g^{-1} for the partial specific volume of the protein, the calculated solvent content is 66.1%. Both the Matthews coefficient and solvent content are well within the normal range expected for protein crystals (Matthews, 1968). An excellent data set to 2.7 Å resolution that has an overall completeness of 95.9% and an R_{sym} of 0.043 (Table 1) has been obtained. The placement of the helium path between the crystal and the beam restricted the measurement of data to 2.7 Å. However, given the high $\langle I\rangle/\langle\sigma(I)\rangle$ value of 13.6 for the outer shell of data, it will in the future be possible to collect significantly higher resolution data for these crystals.

The crystal structure is currently being determined by molecular-replacement techniques. Monomers and dimers of the catalytic subunits of POX, BFD and a model of the catalytic subunit of *E. coli* AHAS II (Ibdah *et al.*, 1996) were all tested as search probes using the program *AMoRe* (Navaza, 1994). A monomeric model that consists of residues 9–161 (α-domain) and 382–521 (γ-domain) from BFD was successful in finding two independent peaks in the rotation search and translation function. Combining these two solutions yielded a plausible dimeric structure. Closer inspection of the two solutions using the graphics program *O* (Jones *et al.*, 1991) did not reveal any interpenetration of symmetry-related molecules and showed reasonable crystal packing contacts. The initial *R* factor for this solution was 0.537 using data in the resolution range 8–4 Å; the structure is currently being refined.

This work was supported by grants ARCS024G and A00105313 from the Australian Research Council (ARC) to RGD and LWG. We thank Dr Harry Tong, Dr Gary Navrotski and Dr Wilfried Schildkamp for assistance at beamline 14C, Advanced Photon Source, Argonne National Laboratory, Chicago, USA. The use of the BioCARS sector was supported by the Australian Synchrotron Research Program, which is funded by the Commonwealth of Australia under the Major National Research Facilities Program. Use of the Advanced Photon Source was supported by the US Department of Energy, Basic Energy Sciences, Office of Energy Research under Contract No. W-31-109-Eng-38. We are grateful to Professor David Chipman, Ben-Gurion University of the Negev, Israel for providing to us the coordinates of the modelled *E. coli* AHAS II structure.

References

Ævarsson, A., Chuang, J. L., Wynn, R. M., Turley, S., Chuang, D. T. & Hol, W. G. (2000). *Structure*, **8**, 277–291.
Ævarsson, A., Seger, K., Turley, S., Sokatch, J. R. & Hol, W. G. J. (1999). *Nature Struct. Biol.* **6**, 785–792.
Arjunan, P., Umland, T., Dyda, F., Swaminathan, S., Furey, W., Sax, M., Farrenkopf, B., Gao, Y., Zhang, D. & Jordan, F. (1996). *J. Mol. Biol.* **256**, 590–600.
Bergfors, T. (1999). *Protein Crystallization. Techniques, Strategies and Tips.* La Jolla, California, USA: International University Line.
Chabrière, E., Charon, M.-H., Volbeda, A., Pieulle, L., Hatchikian, E. C. & Fontecilla-Camps, J.-C. (1999). *Nature Struct. Biol.* **6**, 182–190.
Dobritzsch, D., König, S., Schneider, G. & Lu, G. (1998). *J. Biol. Chem.* **273**, 20196–20204.
Duggleby, R. G. (1997). *Gene*, **190**, 245–249.
Duggleby, R. G. & Pang, S. S. (2000). *J. Biochem. Mol. Biol.* **33**, 1–36.
Dyda, F., Furey, W., Swaminathan, S., Sax, M., Farrenkopf, B. & Jordan, F. (1993). *Biochemistry*, **32**, 6165–6170.
Gollop, N., Damri, B., Barak, Z. & Chipman, D. M. (1989). *Biochemistry*, **28**, 6310–6317.
Hasson, M. S., Muscate, A., McLeish, M. J., Polovnikova, L. S., Gerlt, J. A., Kenyon, G. L., Petsko, G. A. & Ringe, D. (1998). *Biochemistry*, **37**, 9918–9930.
Hershey, H. P., Schwartz, L. J., Gale, J. P. & Abell, L. M. (1999). *Plant Mol. Biol.* **40**,795–806.
Hill, C. M., Pang, S. S. & Duggleby, R. G. (1997). *Biochem. J.* **327**, 891–898.
Ibdah, M., Ahuva, B. I., Livnah, O., Schloss, J. V., Barak, Z. & Chipman, D. M. (1996). *Biochemistry*, **35**, 16282–16291.
Jones, T. A., Zou, J. Y., Cowan, S. W. & Kjeldgaard, M. (1991). *Acta Cryst.* A**47**, 110–119.
Lee, Y.-T. & Duggleby, R. G. (2001). *Biochemistry*, **40**, 6836–6844.
Lindqvist, Y., Schneider, G., Ermler, U. & Sundstrom, M. (1992). *EMBO J.* **11**, 2373–2379.
Matthews, B. W. (1968). *J. Mol. Biol.* **33**, 491–497.
Mendel, S., Elkayam, T., Sella, C., Vinogradov, V., Vyazmensky, M., Chipman, D. M. & Barak, Z. (2001). *J. Mol. Biol.* **307**, 465–477.
Muller, Y. A. & Schulz, G. E. (1993). *Science*, **259**, 965–967.
Navaza, J. (1994). *Acta Cryst.* A**50**, 157–163.
Nikkola, M., Lindqvist, Y. & Schneider, G. (1994). *J. Mol. Biol.* **238**, 387–404.
Ott, K. H., Kwagh, J. G., Stockton, G. W., Sidorov, V. & Kakefuda, G. (1996). *J. Mol. Biol.* **263**, 359–368.
Otwinowski, Z. & Minor, W. (1997). *Methods Enzymol.* **276**, 307–326.
Pang, S. S. & Duggleby, R. G. (1999). *Biochemistry*, **38**, 5222–5231.
Vyazmensky, M., Sella, C., Barak, Z. & Chipman, D. M. (1996). *Biochemistry*, **35**, 10339–10346.
Weinstock, O., Sella, C., Chipman, D. M. & Barak, Z. (1992). *J. Bacteriol.* **174**, 5560–5566.